5-2011

Novel Model for Multispecies Biofilms That Uses Rigid Gas-Permeable Lenses

Rebecca Peyyala
University of Kentucky

Sreenatha S. Kirakodu
University of Kentucky, sreenatha.kirakodu@uky.edu

Jeffrey L. Ebersole
University of Kentucky, jeffrey.ebersole@uky.edu

Karen F. Novak
University of Kentucky, knova2@uky.edu

Novel Model for Multispecies Biofilms That Uses Rigid Gas-Permeable Lenses

Notes/Citation Information
Published in *Applied and Environmental Microbiology*, v. 77, no. 10, p. 3413–3421.

Digital Object Identifier (DOI)
http://dx.doi.org/10.1128/AEM.00039-11

Applied and Environmental Microbiology, May 2011, p. 3413–3421 Vol. 77, No. 10
0099-2240/11/$12.00 doi:10.1128/AEM.00039-11

Novel Model for Multispecies Biofilms That Uses Rigid Gas-Permeable Lenses[▽]

Rebecca Peyyala,* Sreenatha S. Kirakodu, Jeffrey L. Ebersole, and Karen F. Novak

Center for Oral Health Research, College of Dentistry, University of Kentucky, Lexington, Kentucky 40536

Received 4 January 2011/Accepted 10 March 2011

Oral biofilms comprise complex multispecies consortia aided by specific inter- and intraspecies interactions occurring among commensals and pathogenic bacterial species. Oral biofilms are primary initiating factors of periodontal disease, although complex multifactorial biological influences, including host cell responses, contribute to the individual outcome of the disease. To provide a system to study initial stages of interaction between oral biofilms and the host cells that contribute to the disease process, we developed a novel *in vitro* model system to grow biofilms on rigid gas-permeable contact lenses (RGPLs), which enable oxygen to permeate through the lens material. Bacterial species belonging to early- and late-colonizing groups were successfully established as single- or three-species biofilms, with each group comprising *Streptococcus gordonii*, *Streptococcus oralis*, and *Streptococcus sanguinis*; *S. gordonii*, *Actinomyces naeslundii*, and *Fusobacterium nucleatum*; or *S. gordonii*, *F. nucleatum*, and *Porphyromonas gingivalis*. Quantification of biofilm numbers by quantitative PCR (qPCR) revealed substantial differences in the magnitude of bacterial numbers in single-species and multispecies biofilms. We evaluated cell-permeable conventional nucleic acid stains acridine orange, hexidium iodide, and Hoechst 33258 and novel SYTO red, blue, and green fluorochromes for their effect on bacterial viability and fluorescence yield to allow visualization of the aggregates of individual bacterial species by confocal laser scanning microscopy (CLSM). Substantial differences in the quantity and distribution of the species in the multispecies biofilms were identified. The specific features of these biofilms may help us better understand the role of various bacteria in local challenge of oral tissues.

Oral biofilms are complex microbial structures comprising multispecies consortia that are well adapted to live in adverse ecological environments, such as the tooth surface and subgingival sulci in the mouth (4). Oral microorganisms have been reported to demonstrate complex interactions in establishing these biofilms, including specific inter- and intraspecies coaggregation and coadhesion interactions aided by specific adhesion-receptor molecules (26, 52). *In vivo* studies support that individual species in the multispecies oral biofilms are added sequentially, and variation in their accretion leads to differences in composition and spatial distribution (35, 36). These processes in some ways reflect the *in vivo* observations of changes in proportions of proposed pathogenic species related to the initiation of periodontal disease (31, 43). However, characteristics of host responses to these biofilms and the complex multifactorial biological influences also contribute to the individual outcome of disease (26, 29). Bacteriological studies using various techniques have identified a sequence of bacteria that colonize the subgingival sulcus, and somewhat distinctive ecologies are consistent with periodontal health, gingivitis, and periodontopathic biofilms (48, 49). In particular, Gram-positive bacteria are pioneer colonizers, including *Streptococcus gordonii*, *Streptococcus oralis*, *Streptococcus sanguinis*, and other viridans group streptococci, as well as *Actinomyces* spp. As gingival inflammation develops and progresses, a range of Gram-negative bacteria emerge in the oral biofilms, including *Fusobacterium nucleatum*, which plays an important role as a bridging microorganism between several species (24), and *Porphyromonas gingivalis*, a late-colonizing species consistent with adult periodontitis (18).

Development of *in vitro* models of bacterial interactions with host cells is necessary to elucidate more clearly the molecular interactions that take place at the interface between biofilms and host cells during periodontal disease. Single- and multispecies biofilms have been grown in devices such as flow cells and chemostats on static support matrices, such as enamel chips, hydroxyapatite disks, or glass slides (47). Of the various culture systems available, flow-cell models, in conjunction with confocal laser scanning microscopy (CLSM) and fluorescent *in situ* hybridization (FISH), and immunofluorescence staining have been widely used for visualization, differentiation, and spatial distribution of individual species in *in vitro*-grown biofilms of oral bacteria using various model systems (1, 6). Multiple staining of biofilms by FISH is the most widely used technique for species differentiation (50). However, limitations of this technique include several hybridization procedures and sample dehydration, which may introduce artifacts (14, 33), lack of specific discriminatory probes for closely related bacterial species with conserved 16S rRNA genes (12), and uneven staining due to less probe penetration into lower regions of biofilms. Additional investigations have directly used fluorescently labeled antibodies specific for bacterial species to identify the characteristics and distribution of individual species within complex biofilms (6, 39). Recently spatial arrangement of bacteria in biofilms have employed classically available nucleic acid stains for imaging the biofilms (3), although in most cases these stains have been used to characterize the organization of stained bacteria that have been processed through a coaggregation model of bacterial accretion in biofilms, rather

* Corresponding author. Mailing address: Center for Oral Health Research, College of Dentistry, 414 HSRB, 1095 VA Drive, Lexington, KY 40536-0305. Phone: (859) 323-0281. Fax: (859) 257-6566. E-mail: rpeyy1@email.uky.edu.

▽ Published ahead of print on 18 March 2011.

TABLE 1. Primers used in qPCR

Bacteria	Gene	Primers	Annealing temp (°C)	Product size (bp)
S. gordonii	*gtfG*	CTATGCGGATGATGCTAATCAAGTG GGAGTCGCTATAATCTTGTCAGAAA	70	440
S. oralis	*gtfR*	TCCCGGTCAGCAAACTCCAGCC GCAACCTTTGGATTTGCAAC	66	374
S. sanguinis	*gtfP*	GGATAGTGGCTCAGGGCAGCCAGTT GAACAGTTGCTGGACTTGCTTGTC	70	313
S. gordonii	16S	CCATAGACTGTGAGTTGCGAAC CCGTCCCTTTCTGGTAAGATAC	50	427
P. gingivalis	16S	AGGCAGCTTGCCATACTGCG ACTGTTAGCAACTACCGATGT	60	404
F. nucleatum	16S	AGAGTTTGATCCTGGCTCAG GTCATCGTGCACACAGAATTGCTG	60	360
A. naeslundii	16S	CGCGGCCTATCAGCTTGTTG CCGTACTCCCCAGGCGGGG	68	643
Universal	16S	GATTAGATACCCTGGTAGTCCAC TACCTTGTTACGACTT	52	733

than the active growth of the bacteria in developing complex biofilms (10, 27).

These model systems and *in situ* characterization of the structural organization of biofilms have various methodological constraints, and none have yet been effectively used to examine the interactions of viable host cells with these biofilms. For this reason, our lab developed an *in vitro* model system to grow biofilms on rigid gas-permeable hard contact lenses (RGPLs) which will enable examination of their interaction with substratum-bound epithelial cells, or other host cell types, by allowing equilibration of the cocultures with the gaseous environment, whether that be aerobic, microaerophilic, or anaerobic, due to the permeability of the lens material. This report describes characteristics of the methods employed and initial data describing the single and multispecies biofilms created for this novel experimental model. Single- or three-species biofilms, with each group comprising *S. gordonii*, *S. oralis*, and *S. sanguinis* or *S. gordonii*, *A. naeslundii*, and *F. nucleatum* or *S. gordonii*, *F. nucleatum* and *P. gingivalis*, representing early-, middle-, and late-colonizing groups, are developed on RGPL.

MATERIALS AND METHODS

Bacteria and culture conditions. All bacterial strains used in this study (Table 1) were obtained from the ATCC except *Porphyromonas gingivalis* (FDC381). *P. gingivalis*, *Fusobacterium nucleatum* ATCC 25586, *Actinomyces naeslundii* ATCC 49840, and *Streptococcus gordonii* ATCC 10558 were cultured in brain heart infusion (Becton Dickinson and Company, Sparks, MD) medium supplemented with 5 μg hemin ml^{-1} and 1 μg menadione ml^{-1} under anaerobic conditions (85% N_2, 10% H_2, 5% CO_2) at 37°C. *S. sanguinis* ATCC 10556 and *S. oralis* ATCC 10557 were grown in Trypticase yeast extract salts (TYS) medium under anaerobic conditions.

Biofilm growth conditions. Biofilms were grown on rigid gas-permeable lenses (RGPL) (Advanced Vision Technologies, Golden, CO). Prior to biofilm formation, RGPLs were coated with 1% fetal bovine serum (FBS) (Invitrogen) and incubated at room temperature until dry. For single-species biofilms, 5-ml samples of planktonic cultures at an optical density at 600 nm (OD_{600}) of 0.3, grown in their respective media, were added to each RGPL in a single well of a 6-well polystyrene tissue culture plate (BD Falcon, Franklin Lakes, NJ) and incubated in an anaerobic chamber for 3 days. Each day, spent medium was replenished by fresh medium. For multispecies biofilms, planktonic cultures adjusted to an OD_{600} of 0.3 were mixed in equal volumes to obtain a final OD_{600} of 0.3. Five ml of the mixed-species culture was added to each RGPL and grown for 1 day. All multispecies biofilms were grown in supplemented brain heart infusion (BHI) medium.

qPCR analysis of biofilms. Bacterial DNA was isolated by adding 50 μl of alkaline polyethylene glycol directly to the biofilms adherent to the RGPL (6). Real-time quantitative PCR (qPCR) was performed using a LightCycler 2.0 (Roche). Each PCR was performed in a total volume of 20 μl containing 2 μl of 10× LightCycler FastStart DNA Master SYBR green I, 0.5 μM (each) high-performance liquid chromatography (HPLC)-purified forward and reverse primers (Table 1), 4 mM $MgCl_2$, and 100 ng of template DNA. Real-time PCR was carried out with the initial incubation of 10 min at 95°C followed by 45 cycles consisting of denaturing for 95°C for 10 s and annealing for 5 s (Table 1) followed by amplification at 72°C for *X* sec, where *X* is the amplification time [approximately (product size/25) s]. At the end of each cycle, fluorescent product was detected (22). Standard curves were generated for all the target bacteria using DNA from pure cultures. Quantification of the individual target bacteria from the experimental samples was calculated using the standard curves. 16S rRNA primers were used for bacteria from single-species biofilms, and *Streptococcus gtf* gene primers (19) were used for multispecies biofilms involving *Streptococcus* species.

Biofilm staining using fluorescent dyes. Single-species biofilms were stained with nucleic acid stains using the BacLight Live/Dead viability kit containing a solution of 1.67 μM SYTO 9 (green fluorescence) and 10 μM propidium iodide (red fluorescence) (Molecular Probes, Eugene, OR). A 10-μl mixture was added to the biofilms and incubated in the dark for 15 min at room temperature prior to visualization by confocal laser scanning microscopy (CLSM). SYTO 9 stain labels all bacteria green, whereas propidium iodide labels nonviable bacteria with compromised membranes.

Bacterial cultures were also stained with various concentrations of the nucleic acid stains acridine orange (AO), hexidium iodide (HI), and Hoechst 33258 in order to obtain optimal fluorescence with minimum loss of cell viability. A stock solution of AO (Fisher Scientific Co., Fair Lawn, NJ) was prepared at 10 mg ml^{-1} in water, a stock solution of HI (Sigma Aldrich, St. Louis, MO) at 5 mg ml^{-1} in dimethyl sulfoxide, and a stock solution of Hoechst 33258 (Sigma Aldrich, St. Louis, MO) at 10 mg ml^{-1} in DMSO. Cell viability and fluorescence were measured at 0, 6, and 24 h for *F. nucleatum*, *A. naeslundii*, and *S. gordonii* stained with 1, 5, or 10 μg ml^{-1} culture of AO, 2.5, 5, or 10 μg ml^{-1} of HI, and 10, 20, or 30 μg ml^{-1} of Hoechst 33258. Prior to recording cell density and fluorescence, cells were stained for 30 min in the dark, centrifuged to remove

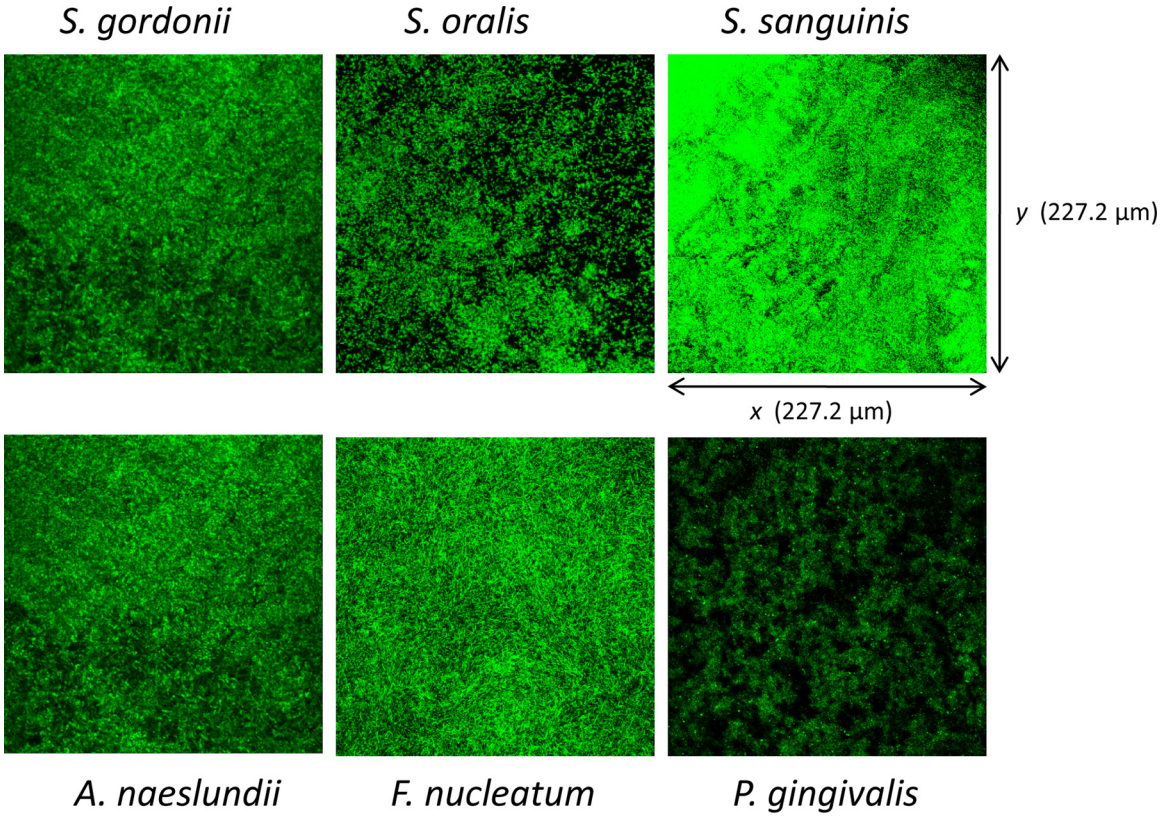

FIG. 1. Analysis of single species *in situ* biofilms on rigid gas permeable contact lens (*x-y* sections) by confocal laser scanning microscopy. Three-day-old biofilms were stained with the Live/Dead bacterial viability kit. Live cells are stained with SYTO 9 and are shown in green. Each representative image is a compilation of 30 optical sections in the *x-y* plane from the substratum to the top of the biofilm.

unincorporated dye, and resuspended in fresh media. Cell density was measured spectrophotometrically (Spectronic 20 Genesys; Sigma-Aldrich, St. Louis, MO) as OD_{600}, and fluorescence intensity was measured using a SpectraMax M2 (Molecular Devices, Sunnyvale, CA) with the excitation and emission wavelengths listed in Table 1. Additional studies were conducted by labeling individual species for examination of multispecies biofilms, *S. gordonii*, *A. naeslundii*, *F. nucleatum*, and *P. gingivalis* with SYTO nucleic acid stains with red (SYTO 17, 59, 60, 61, 62, 63, 64), blue (SYTO 40, 41, 42, 43, 44, 45), and green (SYTO 11, 12, 13, 14, 16, 21, 24, 25) spectra to identify those that gave maximum fluorescence values with minimal loss in cell viability as measured by OD_{600} values 24 h after staining. *S. gordonii* was chosen as a representative of the three oral streptococcal strains for these studies. To each 5 ml of bacterial culture at an OD_{600} of 0.3, individual stains were added at the rate of 10 μg ml^{-1} culture; the cultures were incubated for 30 min at room temperature and centrifuged to remove excess stain, and bacterial pellets were resuspended in BHI media with supplements. The cultures were then incubated in an anaerobic chamber at 37°C in the dark to avoid photobleaching. The maximum duration of incubation chosen for this study was 24 h, as loss of fluorescence occurred beyond 24 h due to subculturing of the bacteria. At 0, 6, and 24 h after incubation, optical density and fluorescence values were measured.

Prior to multispecies biofilm formation, each species was labeled with their respective stains as described above. An equal volume of each culture at an OD_{600} of 0.3 was mixed together to give a combined OD_{600} value of 0.3. The biofilms were formed as described above, but the duration was limited to a single day due to loss of fluorescence intensity.

CLSM imaging. CLSM was performed using a Leica AOBS TCS SP5 confocal laser scanning microscope (Leica, Heidelberg, Germany) equipped with an Argon-Krypton laser with a Leica DMI 6000 CS inverted light microscope and an HCX PL APO 63×/1.30 oil-immersion objective. Thirty fluorescent optical sections were collected in the *z*-plane spanning the full depth of the biofilms. For each set of biofilms, two lenses with three representative areas per lens were scanned. The software used for visualization was LAS AF 2.0 build (Leica, Heidelberg, Germany).

RESULTS

Monospecies biofilm formation. Initially, the bacteria biofilms were evaluated by growth on different conditioning substrates, such as whole saliva, fibronectin, 100% FBS, 10% FBS, or 1% FBS under anaerobic conditions. Biofilm development on RGPL conditioned with 1% FBS was comparable to whole saliva conditioning and was shown to yield better biofilms than the other conditioning treatments (results not shown).

Figure 1 shows representative *x-y* images of 3-day-old monospecies biofilms by confocal laser scanning microscopy stained with the Live/Dead viability stain. The images show only the green fluorescence emitted by SYTO 9, which is a fluorescent marker that stains live cells. Each of the species tested was capable of adhering to RGPL coated with 1% FBS and developed substantial biofilms, although the depth and the biomass of the biofilms did not vary greatly across the various species examined. As an example, the depths of the biofilms in the *z*-plane were 13 μm, 12.85 μm, and 10.75 μm for *S. gordonii*, *S. oralis*, and *S. sanguinis*, respectively.

To complement these visual assessments and to compare biofilms across experiments, qPCR was performed to determine the absolute numbers of bacteria on each RGPL. The average number and range of bacteria per RGPL for each of the monospecies biofilms is shown in Table 2. The results indicate that the numbers of bacteria in the biofilms produced by individual species were highly reproducible as shown by the

TABLE 2. Average number of cells in *S. gordonii*, *S. oralis*, *S. sanguinis*, *A. naeslundii*, *F. nucleatum*, and *P. gingivalis* biofilms[a]

Single-species biofilm	No. of input bacteria/ RGPL (mean × 10^8)	No. of bacteria/RGPL (mean ± SD × 10^8)
S. gordonii	0.68	3.15 ± 1.76
S. oralis	4.73	3.01 ± 1.35
S. sanguinis	4.81	13.90 ± 12.50
A. naeslundii	2.29	5.94 ± 2.91
F. nucleatum	8.15	1.38 ± 0.84
P. gingivalis	11.40	16.10 ± 3.37

[a] Results were derived from triplicate RPGL determinations from three independent experiments from nine replications estimated by quantitative PCR. Input bacteria denotes the amount of bacteria that were inoculated to seed the RGPL biofilms.

variance of the replicates. These results also suggested that all bacterial species used in this study were capable of adhering to 1% FBS-coated RGPL and formed mature biofilms with reproducible numbers of bacteria, although there were substantial differences in the magnitude of bacterial numbers related to the individual species. Comparison of the input bacterial levels to the concentration in the mature biofilms also provided evidence of variation among the species tested. As such, *S. gordonii*, *S. sanguinis*, *A. naeslundii*, and *P. gingivalis* increased by 1.5- to 5-fold during the growth of the biofilms. In contrast, *S. oralis* did not show a measurable increase and *F. nucleatum* demonstrated a pattern whereby approximately 25% of the input bacteria were incorporated into the biofilms.

Multispecies biofilm formation. Visualization of multispecies oral biofilms with single-species resolution required labeling individual species with a distinct fluorophore. For this purpose, cell-permeable conventional nucleic acid stains were compared with novel SYTO dyes for their applicability in live-cell staining. Commonly used nucleic acid stains hexidium iodide, Hoechst 33342, and acridine orange, emitting red, blue, and green fluorescence, respectively, were compared with SYTO dyes with similar fluorescence spectra. The performance of each dye was evaluated based on cytotoxicity and fluorescence intensity for the intact bacteria. Among nucleic acid stains widely used, acridine orange was the least toxic and yielded an observable fluorescence signal with Gram-positive bacteria, *S. gordonii*, and *A. naeslundii*, whereas the fluorescent signal was undetectable with *F. nucleatum* (Fig. 2). Staining with hexidium iodide substantially inhibited the growth of Gram-positive bacteria with moderate fluorescence values (Fig. 2). Although Hoechst 33342 did not inhibit the growth of the bacteria, it provided a limited fluorescent signal for all the bacteria tested. Taking these findings into account, these dyes generally were found not to be useful for labeling individual species and allowing them to grow and accumulate on the RPGL to form *de novo* biofilms.

SYTO dyes were then investigated for their ability to fluoresce with the bacteria, as well as allowing continued growth of the microorganisms (Fig. 3). Significantly improved fluorescence intensities were obtained with the SYTO stains, with the red and blue dyes showing minimal toxicity. Fluorescence intensity varied considerably among the SYTO stains. Table 3 summarizes the optimum optical density and fluorescence intensity for specific red, blue, and green stains. These findings allowed us to identify specific functional stains with which to label each species used in the multispecies biofilms evaluated in this study. The SYTO stains have negligible species specificity; thus, each bacterial cell suspension was prestained before the multispecies biofilms were formed to enable species-specific evaluation of the multiple bacteria.

Confocal images of *S. oralis* (SYTO 44, blue), *S. sanguinis* (SYTO 21, green), and *S. gordonii* (SYTO 17, red) multispecies biofilms (Fig. 4A and B) showed preferential adherence of *S. gordonii* to the FBS-coated RGPL and appeared to form the initial anchoring layer for accumulation of *S. oralis* and *S. sanguinis*. *S. oralis* increased in the *z*-axis toward the central parts of the biofilms (Fig. 4B) and *S. sanguinis* colonized more intensely toward the outer layer. Real-time qPCR using species-specific primers yielded relative amounts of each species. The results in Table 4 show that *S. sanguinis* accounted for approximately 95% of the biofilm bacteria with *S. gordonii* (2%) and *S. oralis* (2%) at much smaller amounts in this streptococcal multispecies biofilm. Confocal images of *A. naeslundii* (SYTO 44, blue), *F. nucleatum* (SYTO 24, green), and *S. gordonii* (SYTO 17, red) multispecies biofilms are shown in Fig. 4C and D. The images show an initial layer of *S. gordonii*, followed by accumulation of *A. naeslundii* and then *F. nucleatum* toward the top region of the biofilms (Fig. 4D). *A. naeslundii* comprised 63% of the biofilm mass, with *S. gordonii* at 29% and *F. nucleatum* at 8% (Table 4). Confocal images of *P. gingivalis* (SYTO 44, blue), *F. nucleatum* (SYTO 24, green), and *S. gordonii* (SYTO 17, red) three-species biofilms are de-

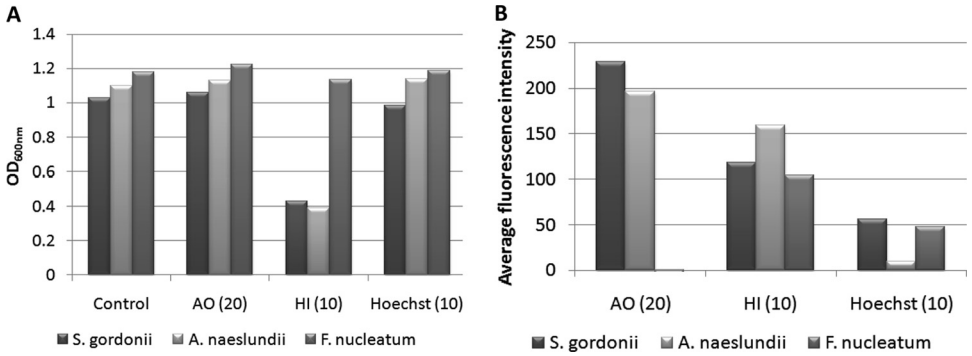

FIG. 2. Optical density and average fluorescence intensity values for *S. gordonii*, *A. naeslundii*, and *F. nucleatum* planktonic cultures stained with acridine orange (20 μg ml^{-1}), hexidium iodide (10 μg ml^{-1}), and Hoechst 33258 (10 μg ml^{-1}) at 24 h.

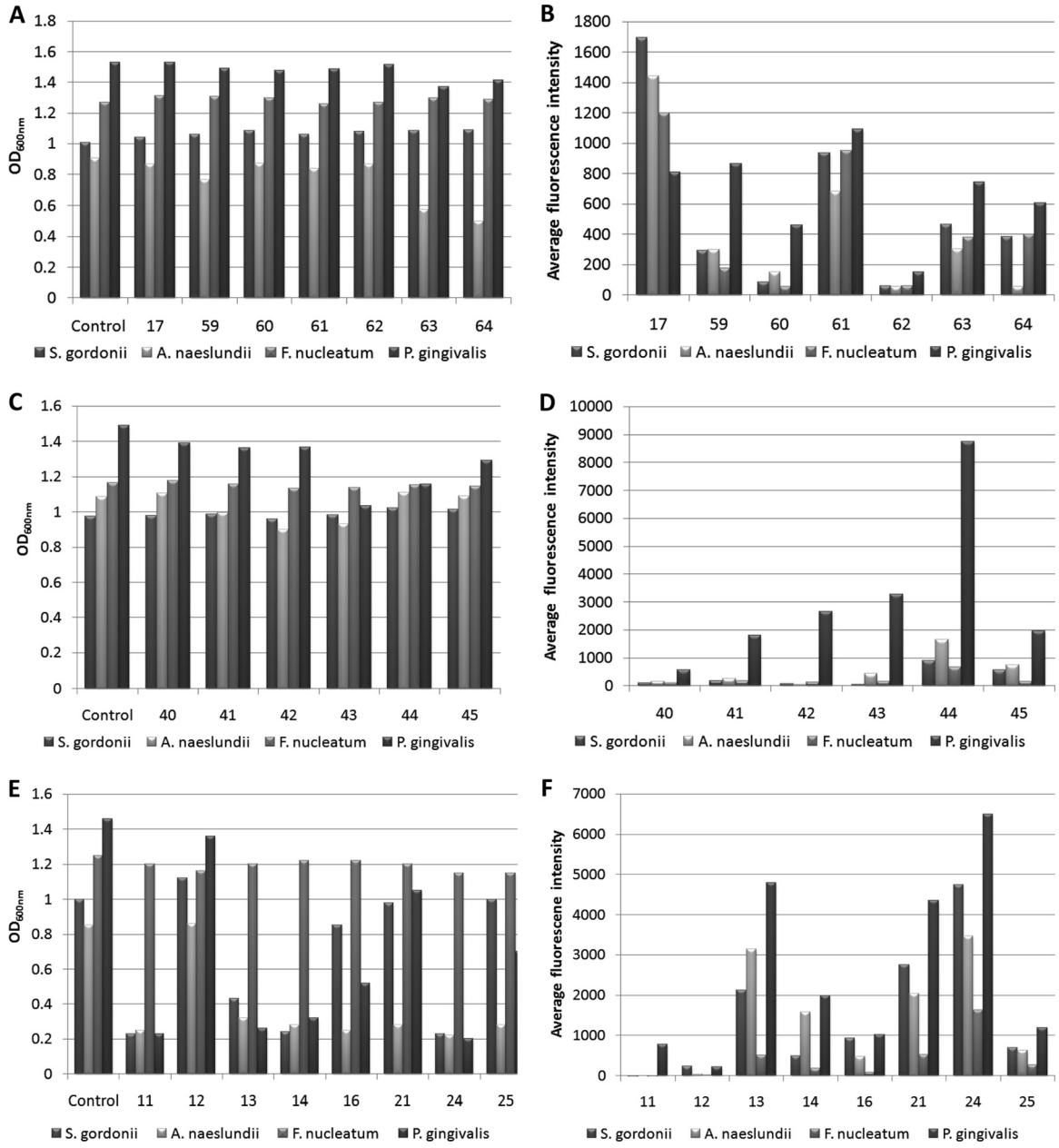

FIG. 3. Cell viability and relative fluorescence intensities of *S. gordonii*, *A. naeslundii*, *F. nucleatum*, and *P. gingivalis* planktonic cultures stained with red, blue, and green SYTO nucleic acid sampler kits. Shown are OD_{600} values and average fluorescence values, respectively, for SYTO red sampler stains (A and B), SYTO blue sampler stains (C and D), and SYTO green sampler stains (E and F). Fluorescence emission was measured in arbitrary units.

TABLE 3. Bacterial strains and their respective nucleic acid stains assigned in three-species biofilms

Biofilm	Bacterium (stain) indicated by color:		
	Red	Blue	Green
1	*S. gordonii* (SYTO 17)	*S. oralis* (SYTO 44)	*S. sanguinis* (SYTO 21)
2	*S. gordonii* (SYTO 17)	*A. naeslundii* (SYTO 44)	*F. nucleatum* (SYTO 24)
3	*S. gordonii* (SYTO 17)	*P. gingivalis* (SYTO 44)	*F. nucleatum* (SYTO 24)

picted in Fig. 4E and F. As in the previous biofilms, an initial layer of *S. gordonii* was observed that comprised 92% of the biofilm bacterial mass. *F. nucleatum* colonized the middle region of the biofilms (2%), with *P. gingivalis* forming the top layer at 6% of the total bacterial numbers (Table 4).

DISCUSSION

It is well recognized that the complex of bacteria that colonize the oral cavity distribute in somewhat distinctive biofilms reflecting the various ecological niches and environments (9).

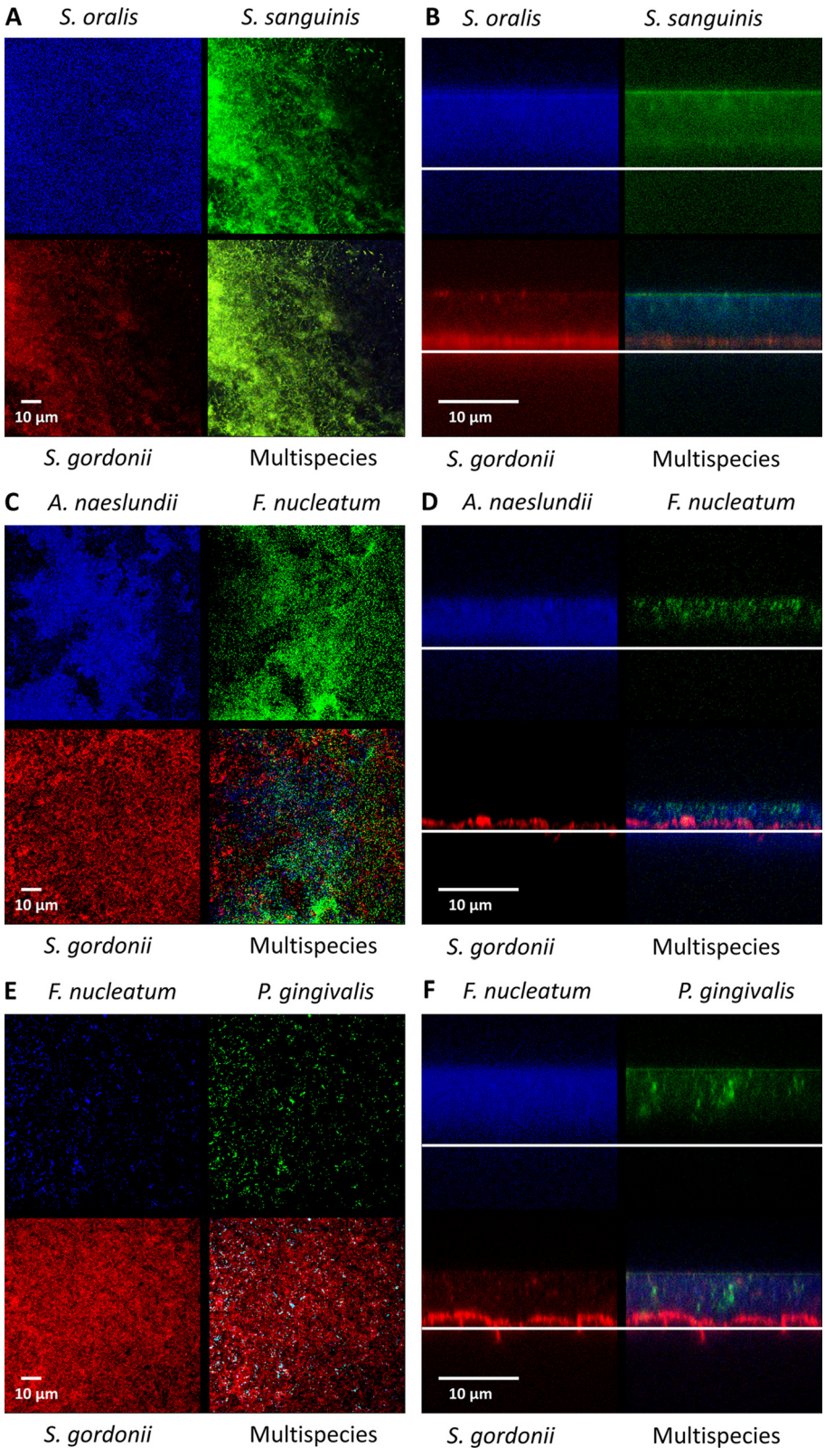

FIG. 4. Comparison of coaggregate inoculated three-species *in situ* biofilms on rigid gas-permeable contact lens by confocal laser scanning microscopy. Each individual species within the three-species biofilms was labeled with the designated SYTO stain prior to mixing. The figures show strain designation above or below each panel. The fourth panel in each set is an overlay of confocal images a, b, and c; the confocal images are of *S. gordonii* (red), *S. oralis* (blue), and *S. sanguinis* (green) in the *x-y* plane (A) and the *x-z* plane (B); *S. gordonii* (red), *A. naeslundii* (blue), and *F. nucleatum* (green) in the *x-y* plane (C) and the *x-z* plane (D); and *S. gordonii* (red), *F. nucleatum* (blue), and *P. gingivalis* (green) in the *x-y* plane (E) and the *x-z* plane (F). The white lines denote the approximate position of the RGPL.

TABLE 4. Mean and relative composition of individual species in mixed-species biofilms[a]

Biofilm	Mean ± SEM of individual species/RGPL biofilms (%)					
	S. gordonii	*S. oralis*	*S. sanguinis*	*A. naeslundii*	*F. nucleatum*	*P. gingivalis*
1	$3.17 \pm 2.41 \times 10^5$ (2.18)	$3.23 \pm 1.53 \times 10^5$ (1.99)	$1.82 \pm 0.45 \times 10^7$ (95.82)			
2	$4.84 \pm 0.45 \times 10^8$ (29.25)			$1.06 \pm 0.15 \times 10^9$ (62.87)	$1.35 \pm 0.35 \times 10^8$ (7.88)	
3	$3.25 \pm 2.10 \times 10^9$ (91.81)				$7.54 \pm 5.60 \times 10^7$ (1.76)	$1.45 \pm 0.59 \times 10^8$ (6.43)

[a] Data are derived from three replicates.

Moreover, extensive research has been conducted over the last decade in attempts to recapitulate these biofilms, *in vitro*, with goals to evaluate interbacterial interactions based upon cognate recognition leading to coaggregation (26), physiological interdependencies (27), and targeted gene regulation within the individual species that enhance their capacity to colonize, survive, and replicate in this complex microbial ecology (42). However, much less information is available that translates these ecological findings into studies related to characteristics of host responses to the microbial complexes (16). Consequently, we developed a model system for creating mono- and multispecies biofilms on rigid gas-permeable contact lens (RPGL) material. Clearly, the clinical aspects of the lenses support bacteria colonizing this material as an undesired side effect that requires routine treatment of RPGL. Additionally, clinically relevant improvements in the material have focused on a greater capacity of the lenses to increase environmental atmosphere transfer to the underlying corneal tissues, thus enhancing the "wearability" of the lenses. These properties enabled us to evaluate the characteristics of the accumulation of oral bacteria in biofilms using confocal microscopy, with a goal of analyzing the interaction of these biofilms with host cells.

To accomplish this initial task, we required low-toxicity and stable fluorescent stains to image the structure of the multispecies biofilms on the RGPL. An important aspect of this approach was a requirement for the bacteria to continue to survive and replicate following staining by the dyes. Traditional nucleic acid stains, such as acridine orange, hexidium iodide, and Hoechst 33342, have been used to stain multiple species of planktonic and biofilm bacteria for visualization using standard fluorescent microscopy (21, 46) and confocal laser scanning microscopy (10, 27). However, generally these have been used as terminal analytical approaches for bacterial counts and/or viability (30, 45) or to provide an evaluation of bacterial aggregation onto solid surfaces (10, 27) with minimal assessment for visualizing and maintaining cell viability. Our approach required that the fluorescent-labeled species continue to maintain sufficient fluorescent intensity and the ability to replicate over a 24-h interval required to actually "mature" into structured biofilms.

SYTO dyes are novel cell-permeable nucleic acid stains that can be excited in the UV or visible light range and are routinely used in live-cell confocal microscopy (53). Although all SYTO stains are homologues, small structural differences account for differences in excitation and emission spectra. SYTO stains are cyanine derivatives and induce low toxicity for mammalian cell cultures (53). SYTO stains are shown to diffuse passively through cell membranes in mammalian cell cultures, although there are minimal reports on bacterial cell permeability. Nevertheless, in bacterial systems it could be speculated that the presence of cell walls would hinder the diffusion of SYTO stains, which could in turn affect the internal accumulation, binding to nucleic acids, and fluorescence intensity. Moreover, structural differences of SYTO stains also affect relative affinities for nucleic acids and fluorescence enhancement upon binding to nucleic acids. Although SYTO dyes have been used most notably as viability stains and for flow cytometric applications in eukaryotic cell systems (54), their potential for use in bacterial biofilm visualization has not fully explored except for a few SYTO dyes from the red subfamily that have been used mainly as nonspecific bacterial stains (32). A series of SYTO dyes belonging to red, blue, and green spectra were tested to determine the optimal dye for staining Gram-positive and Gram-negative oral bacterial species. Pronounced differences in fluorescence signal were observed across bacterial species and SYTO dyes tested, although the SYTO stains gave substantially higher fluorescence intensities than acridine orange, Hoechst 33342, or hexidium iodide. This is likely accounted for by the SYTO stains performing as whole-cell nucleic acid stains compared to the nucleic acid stains, which are DNA selective. In mammalian cells, it has been suggested that there is gradient-dependent SYTO dye uptake by organelles such as mitochondria, ER, and Golgi apparatus (51, 53).

Although SYTO dyes have been shown to present low cytotoxicity in mammalian cell cultures (53), in our study, some SYTO dyes did have a substantial impact on bacterial cell viability, fundamentally being either bacteriostatic or bactericidal for selected species. Thus, the small structural differences among the SYTO dyes appear to be sufficient to alter their cytotoxic potential. Because of these studies we were able to identify selected SYTO dyes for the range of bacterial species that would enable replication of the bacteria, as well as maintaining sufficient intensity to visualize with confocal microscopy.

Using these results, we documented unique characteristics of multispecies biofilms created on the RGPL using strains of oral bacteria representative of the various species that have been identified in the human oral cavity. Visually, the stained biofilms provided spatial distribution of individual species in these three-species biofilms that provide some reflection of the reported sequential nature of oral biofilms (48). Our results also showed that the multispecies biofilms grew more rapidly and gave rise to thicker biofilms even though these were grown for only a day compared to the single-species biofilms, which were grown for 3 days. This observation is in agreement with previous reports suggesting that in multispecies biofilms, individual bacterial species benefit from mutualistic beneficial associations, e.g., nutritional, compared to single-species biofilms (2, 37).

Genetically distinct oral bacteria have been shown to adhere to tooth enamel and to one another by several specific adhesin-receptor interactions. Research from various groups demonstrated that members of the *Streptococcus* genus are the early colonizers that anchor the biofilms to saliva-coated substratum *in vitro* and reflect *in vivo* biofilm initiation (11, 34, 35), and, in particular, *S. gordonii* demonstrates this property (8, 17). Intraspecies coaggregation of streptococci has been shown by extensive coaggregation analysis (23); however, in our study, unique sequential deposition of taxonomically related coaggregation partners such as *S. gordonii*, *S. oralis*, and *S. sanguinis* was also observed. Of the three streptococcal species, *S. gordonii* appears to possess mechanisms that more effectively compete with *S. oralis* and *S. sanguinis* in adhering to fetal bovine serum (FBS)-coated RGPL. The RGPL were initially treated with FBS, since previous findings have documented the critical nature of fibronectin in serum as a substrate for adherence of oral bacteria, particularly in studies of subgingival ecologies where the sites are bathed by serum, not saliva. We used FBS, which contains high levels of fibronectin and has binding domains similar to those of human fibronectin, since the use of human serum would have been complicated by existing antibodies to various oral bacteria that occur naturally in human serum (13). Various studies have indicated that *S. oralis* bears coaggregation receptors for several other genera of oral bacteria (26), and from these biofilm pictures it appeared that *S. oralis* may have functioned as a bridge between *S. gordonii* and *S. sanguinis*, forming an intermediate layer. This unique preferential biofilm structuring and organization among closely related early-colonizing streptococcal species is a novel finding from these studies.

A. naeslundii and *S. gordonii* have demonstrated complex interactions, where *A. naeslundii* benefits the growth of *S. gordonii* (20). This is consistent with our observations where *S. gordonii* and *A. naeslundii* showed preferential binding in the biofilms. Moreover, as *A. naeslundii* also bears multiple receptors that contribute to bacterial coaggregation with various oral genera (7, 44), it appeared to function as a bridge between *S. gordonii* and *F. nucleatum*. Similarly, it can be speculated that adhesin-bearing *F. nucleatum* bacteria functioned as a bridge between early-colonizing *S. gordonii* and late-colonizing *P. gingivalis* on the RPGL biofilms by cognate interaction through specific receptors. Another consistent observation of this study is that in all the mixed-species biofilms, the bacterial species created an organized structure that would be predicted based upon both *in vitro* planktonic interactions (26) and *in vivo* observations of the development of biofilms from health to gingivitis to periodontitis (48, 49).

The capacity for bacteria to develop oral biofilms has been related to the ability of various genera and species of oral bacteria to coaggregate (25). These intergeneric coadhesion events have been implicated in various aspects of the formation of complex oral microbial biofilms, including the structure, nutritional symbiosis, interspecies communication, and sharing of genetic material (25, 26, 38, 40, 41). It is clear from the literature that a number of the species that were employed in developing these biofilms have the potential to coaggregate; however, there are no direct data for some of the strains that were used (5, 15, 26, 28). One study by Foster and Kolenbrander (15) suggested that with *Veillonella atypica* and *A. naeslundii*, coaggregation in the planktonic phase affected biofilm formation. Although coaggregates of the three species may have formed before inoculation of RGPL, this model was designed to create multispecies biofilms for challenge of host cells. Thus, within the context of this goal each species aligned itself and/or replicated in the biofilm architecture, enabling studies to characterize the host response to the complex ecologies. These seminal findings demonstrate that we have developed a unique *in vitro* model system to study biofilm formation. This model system showed reproducible biofilms that will enable studies of various host cell responses, including those of epithelial cells and immune cells, to document specific patterns of responses to structured oral bacterial biofilms.

ACKNOWLEDGMENTS

This work was supported by NIH/NIDCR grant R21DE018177.

We thank the confocal and electron microscopy imaging facility of University of Kentucky and staff Mary G. Engle and James G. Begley for their valuable technical assistance. We also thank Jonathan Bott and Aaron Rose for their valuable help with the study.

REFERENCES

1. **Al-Ahmad, A., et al.** 2009. Bacterial colonisation of enamel in situ investigated with fluorescence in situ hybridization (FISH). J. Med. Microbiol. **58:**1359–1366.
2. **Brown, S. A., and M. Whiteley.** 2007. A novel exclusion mechanism for carbon resource partitioning in Aggregatibacter actinomycetemcomitans. J. Bacteriol. **189:**6407–6414.
3. **Capestany, C. A., et al.** 2006. Role of the Porphyromonas gingivalis InlJ protein in homotypic and heterotypic biofilm development. Infect. Immun. **74:**3002–3005.
4. **Carlsson, J.** 1997. Bacterial metabolism in dental biofilms. Adv. Dent. Res. **11:**75–80.
5. **Chalmers, N. I., R. J. Palmer, Jr., J. O. Cisar, and P. E. Kolenbrander.** 2008. Characterization of a Streptococcus sp.-Veillonella sp. community micromanipulated from dental plaque. J. Bacteriol. **190:**8145–8154.
6. **Chomczynski, P., and M. Rymaszewski.** 2006. Alkaline polyethylene glycol-based method for direct PCR from bacteria, eukaryotic tissue samples, and whole blood. Biotechniques **40:**454–458.
7. **Cisar, J., A. Sandberg, G. Reddy, C. Abeygunawardana, and C. Bush.** 1997. Structural and antigenic types of cell wall polysaccharides from viridans group streptococci with receptors for oral actinomyces and streptococcal lectins. Infect. Immun. **65:**5035–5041.
8. **Cook, G. S., J. W. Costerton, and R. J. Lamont.** 1998. Biofilm formation by Porphyromonas gingivalis and Streptococcus gordonii. J. Periodontal Res. **33:**323–327.
9. **Costerton, J. W., G. G. Geesey, and K. J. Cheng.** 1978. How bacteria stick. Sci. Am. **238:**86–95.
10. **Daep, C. A., R. J. Lamont, and D. R. Demuth.** 2008. Interaction of Porphyromonas gingivalis with oral streptococci requires a motif that resembles the eukaryotic nuclear receptor box protein-protein interaction domain. Infect. Immun. **76:**3273–3280.
11. **Diaz, P. I., et al.** 2006. Molecular characterization of subject-specific oral microflora during initial colonization of enamel. Appl. Environ. Microbiol. **72:**2837–2848.
12. **Dige, I., H. Nilsson, M. Kilian, and B. Nyvad.** 2007. In situ identification of streptococci and other bacteria in initial dental biofilm by confocal laser scanning microscopy and fluorescence in situ hybridization. Eur. J. Oral Sci. **115:**459–467.
13. **Ebersole, J. L.** 2003. Immune responses in periodontal diseases, p. 111–143. *In* T. G. Wilson, Jr., and K. S. Kornman (ed.), Fundamentals of periodontics, 2nd ed. Quintessence Publishing Co., Inc., Chicago, IL.
14. **Evans, R. P., C. L. Nelson, W. R. Bowen, M. G. Kleve, and S. G. Hickmon.** 1998. Visualization of bacterial glycocalyx with a scanning electron microscope. Clin. Orthop. Relat. Res. **347:**243–249.
15. **Foster, J. S., and P. E. Kolenbrander.** 2004. Development of a multispecies oral bacterial community in a saliva-conditioned flow cell. Appl. Environ. Microbiol. **70:**4340–4348.
16. **Guggenheim, B., et al.** 2009. In vitro modeling of host-parasite interactions: the "subgingival" biofilm challenge of primary human epithelial cells. BMC Microbiol. **9:**280.
17. **Hamada, T., M. Kawashima, H. Watanabe, J. Tagami, and H. Senpuku.** 2004. Molecular interactions of surface protein peptides of Streptococcus gordonii with human salivary components. Infect. Immun. **72:**4819–4826.
18. **Holt, S. C., and J. L. Ebersole.** 2005. Porphyromonas gingivalis, Treponema

denticola, and Tannerella forsythia: the "red complex," a prototype polybacterial pathogenic consortium in periodontitis. Periodontol. 2000 **38:**72–122.
19. **Hoshino, T., et al.** 2004. PCR detection and identification of oral streptococci in saliva samples using gtf genes. Diagn. Microbiol. Infect. Dis. **48:**195–199.
20. **Jakubovics, N. S., S. R. Gill, M. M. Vickerman, and P. E. Kolenbrander.** 2008. Role of hydrogen peroxide in competition and cooperation between Streptococcus gordonii and Actinomyces naeslundii. FEMS Microbiol. Ecol. **66:**637–644.
21. **Jun, H.-K., Y.-M. Kang, H.-R. Lee, S.-H. Lee, and B.-K. Choi.** 2008. Highly conserved surface proteins of oral spirochetes as adhesins and potent inducers of proinflammatory and osteoclastogenic factors. Infect. Immun. **76:** 2428–2438.
22. **Kirakodu, S. S., M. Govindaswami, M. J. Novak, J. L. Ebersole, and K. F. Novak.** 2008. Optimizing qPCR for the quantification of periodontal pathogens in a complex plaque biofilm. Open Dent. J. **2:**49–55.
23. **Kolenbrander, P. E.** 2000. Oral microbial communities: biofilms, interactions, and genetic systems 1. Annu. Rev. Microbiol. **54:**413–437.
24. **Kolenbrander, P. E., R. N. Andersen, and L. V. H. Moore.** 1989. Coaggregation of *Fusobacterium nulceatum*, *Selenomonas flueggei*, *Selenomonas infelix*, *Selenomonas noxia*, and *Selenomonas sputigena* with strains from 11 genera of oral bacteria. Infect. Immun. **57:**3194–3203.
25. **Kolenbrander, P. E., R. J. Palmer, Jr., S. Periasamy, and N. S. Jakubovics.** 2010. Oral multispecies biofilm development and the key role of cell-cell distance. Nat. Rev. Microbiol. **8:**471–480.
26. **Kolenbrander, P. E., et al.** 2006. Bacterial interactions and successions during plaque development. Periodontol. 2000 **42:**47–79.
27. **Kuboniwa, M., et al.** 2009. Proteomics of Porphyromonas gingivalis within a model oral microbial community. BMC Microbiol. **9:**98.
28. **Lamont, R. J., et al.** 2002. Role of the Streptococcus gordonii SspB protein in the development of Porphyromonas gingivalis biofilms on streptococcal substrates. Microbiology **148:**1627–1636.
29. **Landi, L., S. Amar, A. S. Polins, and T. E. van Dyke.** 1997. Host mechanisms in the pathogenesis of periodontal disease. Curr. Opin. Peiodontol. **4:**3–10.
30. **Lang, C., et al.** 2010. Specific Lactobacillus/Mutans Streptococcus co-aggregation. J. Dent. Res. **89:**175–179.
31. **Ledder, R. G., et al.** 2007. Molecular analysis of the subgingival microbiota in health and disease. Appl. Environ. Microbiol. **73:**516–523.
32. **Möhle, R. B., et al.** 2007. Structure and shear strength of microbial biofilms as determined with confocal laser scanning microscopy and fluid dynamic gauging using a novel rotating disc biofilm reactor. Biotechnol. Bioeng. **98:**747–755.
33. **Morck, D. W., et al.** 1987. Electron microscopic description of glycocalyx and fimbriae on the surface of Pasteurella haemolytica-A1. Can. J. Vet. Res. **51:**419–420.
34. **Nobbs, A. H., R. J. Lamont, and H. F. Jenkinson.** 2009. Streptococcus adherence and colonization. Microbiol. Mol. Biol. Rev. **73:**407–450.
35. **Nyvad, B., and M. Kilian.** 1990. Comparison of the initial streptococcal microflora on dental enamel in caries-active and in caries-inactive individuals. Caries Res. **24:**267–272.
36. **Nyvad, B., and M. Kilian.** 1987. Microbiology of the early colonization of human enamel and root surfaces in vivo. Scand. J. Dent. Res. **95:**369–380.
37. **Palmer, R. J., K. Kazmerzak, M. C. Hansen, and P. E. Kolenbrander.** 2001. Mutualism versus independence: strategies of mixed-species oral biofilms in vitro using saliva as the sole nutrient source. Infect. Immun. **69:**5794–5804.
38. **Periasamy, S., N. I. Chalmers, L. Du-Thumm, and P. E. Kolenbrander.** 2009. Fusobacterium nucleatum ATCC 10953 requires Actinomyces naeslundii ATCC 43146 for growth on saliva in a three-species community that includes Streptococcus oralis 34. Appl. Environ. Microbiol. **75:**3250–3257.
39. **Periasamy, S., and P. E. Kolenbrander.** 2009. Aggregatibacter actinomycetemcomitans builds mutualistic biofilm communities with Fusobacterium nucleatum and Veillonella species in saliva. Infect. Immun. **77:**3542–3551.
40. **Periasamy, S., and P. E. Kolenbrander.** 2010. Central role of the early colonizer Veillonella sp. in establishing multispecies biofilm communities with initial, middle, and late colonizers of enamel. J. Bacteriol. **192:**2965–2972.
41. **Periasamy, S., and P. E. Kolenbrander.** 2009. Mutualistic biofilm communities develop with Porphyromonas gingivalis and initial, early, and late colonizers of enamel. J. Bacteriol. **191:**6804–6811.
42. **Rickard, A. H., et al.** 2006. Autoinducer 2: a concentration-dependent signal for mutualistic bacterial biofilm growth. Mol. Microbiol. **60:**1446–1456.
43. **Rocas, I. N., and J. F. Siqueira, Jr.** 2008. Root canal microbiota of teeth with chronic apical periodontitis. J. Clin. Microbiol. **46:**3599–3606.
44. **Ruhl, S., A. L. Sandberg, and J. O. Cisar.** 2004. Salivary receptors for the proline-rich protein-binding and lectin-like adhesins of oral actinomyces and streptococci. J. Dent. Res. **83:**505–510.
45. **Seo, E.-Y., T.-S. Ahn, and Y.-G. Zo.** 2010. Agreement, precision and accuracy of epifluorescence microscopy methods for enumeration of total bacterial number. Appl. Environ. Microbiol. **76:**1981–1991.
46. **Singh, R., et al.** 2003. Microbial diversity of biofilms in dental unit water systems. Appl. Environ. Microbiol. **69:**3412–3420.
47. **Sissons, C. H.** 1997. Artificial dental plaque biofilm model systems. Adv. Dent. Res. **11:**110–126.
48. **Socransky, S., A. Haffajee, M. Cugini, C. Smith, and R. L. Kent.** 1998. Microbial complexes in subgingival plaque. J. Clin. Periodontol. **25:**134–144.
49. **Tanner, A., M. F. J. Maiden, P. J. Macuch, L. L. Murray, and R. L. Kent.** 1998. Microbiota of health, gingivitis, and initial periodontitis. J. Clin. Periodontol. **25:**85–98.
50. **Thurnheer, T., R. Gmür, and B. Guggenheim.** 2004. Multiplex FISH analysis of a six-species bacterial biofilm. J. Microbiol. Methods **56:**37–47.
51. **Vanhecke, D., et al.** 2008. Pseudovacuoles—immobilized by high-pressure freezing—are associated with blebbing in walker carcinosarcoma cells. J. Microsc. **230:**253–262.
52. **Whittaker, C. J., C. M. Klier, and P. E. Kolenbrander.** 1996. Mechanisms of adhesion by oral bacteria. Annu. Rev. Microbiol. **50:**513–552.
53. **Wlodkowic, D., J. Skommer, and Z. Darzynkiewicz.** 2008. SYTO probes in the cytometry of tumor cell death. Cytometry A **73:**496–507.
54. **Wlodkowic, D., J. Skommer, C. Hillier, and Z. Darzynkiewicz.** 2008. Multiparameter detection of apoptosis using red-excitable SYTO probes. Cytometry A **73:**563–569.